Interfacial structure of epitaxial MgB_2 thin films grown on (0001) sapphire

W. Tian and X. Q. Pan[a)]
Department of Materials Science & Engineering, University of Michigan, Ann Arbor, Michigan 48109

S. D. Bu, D. M. Kim, J. H. Choi, S. Patnaik, and C. B. Eom
Department of Materials Science and Engineering, University of Wisconsin, Madison, Wisconsin 27708

(Received 22 March 2002; accepted for publication 30 April 2002)

The microstructure and interfacial atomic structure of MgB_2 thin films fabricated on the (0001) Al_2O_3 substrate were characterized by transmission electron microscopy. It was found that the MgB_2 films grow epitaxially on the substrate with an orientation relationship with respect to the substrate as: $(0001)MgB_2 \| (0001)Al_2O_3$ and $[11\bar{2}0]MgB_2 \| [10\bar{1}0]Al_2O_3$. At the film/substrate interface, both MgO and $MgAl_2O_4$ phases were observed, which also grow epitaxially on the (0001) Al_2O_3 substrate. The formation of these intermediate phases is ascribed to the existence of oxygen during the annealing. © *2002 American Institute of Physics.* [DOI: 10.1063/1.1489101]

The recent discovery of superconductivity above 39 K in intermetallic MgB_2 has resparked interest in nonoxide superconductors from both the fundamental and technical perspectives.[1,2] Among the prominent properties of MgB_2 are the record-breaking transition temperature (T_C) in metallic superconductors and the ability to carry strongly linked current flow.[3–5] Growth of single crystal is of particular importance in probing the fundamental properties of MgB_2, such as the superconducting mechanism and the anisotropy in properties. Unfortunately, a peritectic decomposition of MgB_2 at $\sim$650 °C limits the growth of single crystals from the melt.[6] Growth of epitaxial thin films, on the other hand, paves an alternative way to this end. In addition, epitaxial thin films are themselves technically important given their tremendous opportunities for microelectronic applications.

Despite recent intensive efforts, the growth of MgB_2 epitaxial thin films remains challenging due to the high volatility of Mg in a broad temperature window and the tendency to form MgO in the presence of oxygen. *In-situ* growth has to date only resulted in films composed of multiphase, poor crystallinity in nature, and of relatively low T_C.[7–11] In contrast, *ex-situ* processes involving the annealing of pure boron and MgB_2 films in Mg vapor appeared to be promising.[12–16] Most recently, a successful growth of epitaxial MgB_2 thin films has been achieved by exposing the predeposited boron thin films in Mg vapor at high temperatures.[17,18] Here, we reported a transmission electron microscopy TEM study on the microstructure and interfacial atomic structure of such thin films, representing one of the key steps to understanding its growth mechanism and structure-property relationships.

The MgB_2 thin films were synthesized by annealing the predeposited boron films in Mg vapor in an encapsulated quartz tube. The boron films were deposited on the (0001) Al_2O_3 substrates by rf sputtering. Details of synthesis were reported elsewhere.[17,18] The atomic structure of film/substrate interfaces was studied within a high resolution electron microscope JEOL-4000EX operated at 400 kV, providing a point-to-point resolution close to 0.17 nm. The chemical composition of the film was studied by energy dispersive spectroscopy (EDS) and electron energy-loss spectroscopy (EELS) using a field emission gun analytical electron microscope JEOL-2010F. High-resolution transmission electron microscopy (HRTEM) image simulations were performed using the EMS software.

A well lattice-matched substrate is critical to ensure an epitaxial growth. MgB_2 has a hexagonal structure with space group $P6/mmm$ (No. 191) and lattice constants of $a = 3.086$ and $c = 3.524$ Å at room temperature.[19] Al_2O_3 possesses a hexagonal structure with space group $R\text{-}3C$ (No. 167) and lattice constants of $a = 4.758$ and $c = 12.991$ Å at room temperature.[19] One can see that the basal plane of MgB_2 and Al_2O_3 possess the same six-fold symmetry and an identical atomic configuration. While an *a*-to-*a* alignment between MgB_2 and Al_2O_3 results in $\sim$23% lattice mismatch, being unfavorable for the epitaxial growth, a 30° angular off the *a*-to-*a* alignment, namely $[11\bar{2}0]MgB_2 \| [10\bar{1}0]Al_2O_3$, provides a small lattice mismatched ($\sim$11%) alignment to possibly allow an epitaxial growth.

Low-magnification TEM and electron diffraction studies were performed to examine the overall microstructure as well as to establish the epitaxial orientation relationships. Figure 1(a) is a low-magnification cross-sectional TEM image showing a portion of the film. The film has an average thickness of 400 nm, with a peak-to-valley surface roughness of approximately 80 nm. Figures 1(b) and 1(c) are selected-area electron diffraction patterns recorded from the film and the substrate, respectively. The patterns were recognized as the $[11\bar{2}0]$ zone axis diffraction pattern of hexagonal MgB_2 and the $[10\bar{1}0]$ zone axis diffraction pattern of Al_2O_3. These studies indicated that a MgB_2 thin film grows on the (0001) Al_2O_3 substrate, with epitaxial orientation relationships of $(0001)MgB_2 \| (0001)Al_2O_3$ and $[11\bar{2}0]MgB_2 \| [10\bar{1}0]Al_2O_3$, respectively. Note that there is indeed a 30° angular off the *a*-to-*a* alignment between the basal plane of MgB_2 and the Al_2O_3 substrate. Additionally, two thin layers in the vicinity of the film-substrate interface show noticeably different contrast features from the film, indicating the formation of interfacial microstructures.

To understand the orientation relationship between the

[a)]Author to whom correspondence should be addressed; electronic mail: penx@umich.edu

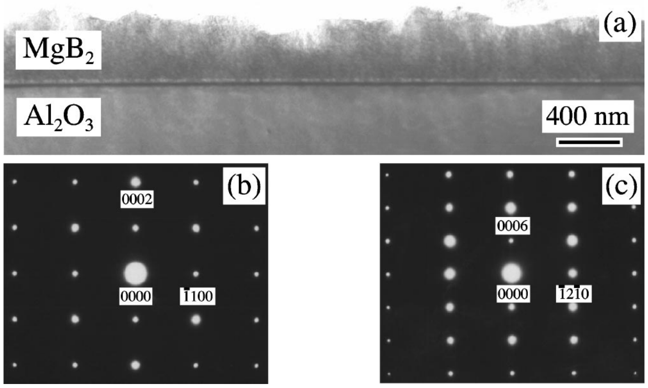

FIG. 1. (a) Low magnification cross-sectional bright-field TEM image of a MgB_2 film grown on the (0001) Al_2O_3 substrate. (b) and (c) selected-area diffraction pattern taken from the film and the substrate with the electron beam incident along the same direction.

MgB_2 film and the (0001) Al_2O_3 substrate, which is important for understanding the growth mechanisms and the physical properties of the film, the interfacial structure was studied using HRTEM technique combined with computer image analysis. Figure 2(a) shows an HRTEM micrograph taken from the film/substrate interface with the incident electron beam aligned along the $[10\bar{1}0]$ zone axis of Al_2O_3. Four layers with distinct structural characteristics are seen. The top layer was determined to be MgB_2, oriented with its $[11\bar{2}0]$ axis parallel to the $[10\bar{1}0]$ direction of Al_2O_3. This study confirms the orientation relationship between MgB_2 and Al_2O_3, revealed by selected area electron diffractions. Between the MgB_2 film and the substrate, two intermediate layers exist, which are unexpected for the overall epitaxial relationship between the film and substrate. Fourier transform studies and computer image simulations revealed that two intermediate layers correspond to the (111) oriented, epitaxial MgO (upper) and the $MgAl_2O_4$ (lower) phase. This

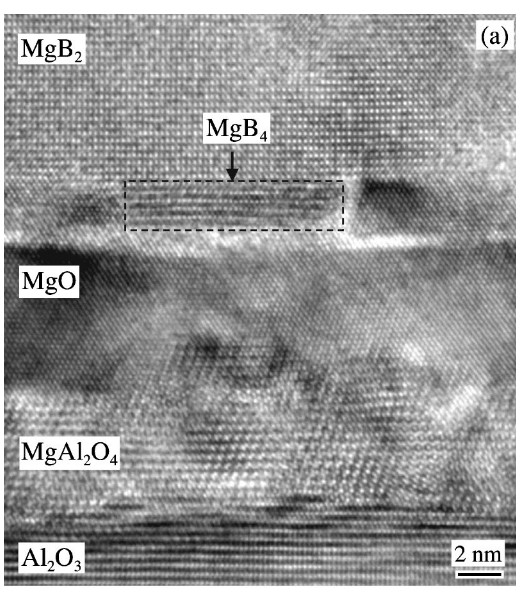

FIG. 2. HRTEM image of the interface between MgB_2 film and the Al_2O_3 substrate along the $[11\bar{2}0]$ zone axis of MgB_2. Interfacial microstructure consisting of MgO and $MgAl_2O_4$ epitaxial layers is seen. An isolated thin layer composed of MgB_4 is also seen at the interface as indicated by the dashed line box.

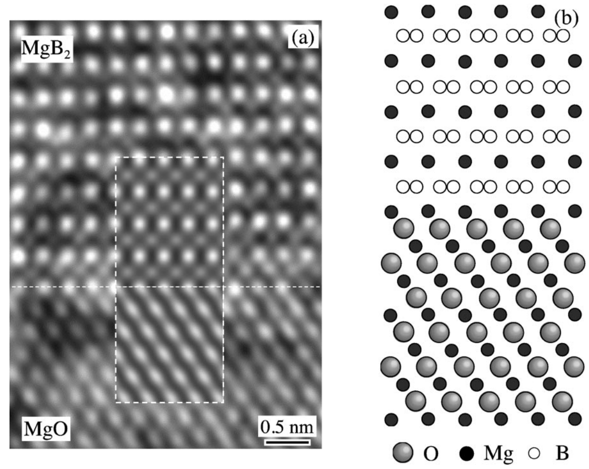

FIG. 3. (a) HRTEM image of the MgB_2–MgO interface with the imaging electron beam along the $[11\bar{2}0]$ direction of MgB_2. The insert in the middle is a computer simulated image (thickness $=3$ nm and defocus $=-50$ nm) that optimally fits the experimental one. (b) An atomic structure of the interface deduced from the HRTEM and computer simulations.

conclusion is further confirmed by spatially resolved x-ray EDS and EELS. Detailed TEM studies showed that the intermediate layers (MgO and $MgAl_2O_4$) are continuous along the film/substrate interface, in which $MgAl_2O_4$ layer lies underneath the MgO layer. Both MgO and $MgAl_2O_4$ grow epitaxially on the Al_2O_3 substrate, with orientation relationship of

$$(0001)[11\bar{2}0]MgB_2 \| (111)[1\bar{1}0]MgO \| (111)$$

$$[1\bar{1}0]MgAl_2O_4 \| (0001)[10\bar{1}0]Al_2O_3.$$

The orientation relationships between MgO and Al_2O_3 established here are similar with those found in the MgO films grown on the (0001) Al_2O_3 substrate by molecular beam epitaxy,[20] except that no twin variants were observed in the present MgO layer. In addition to the epitaxial MgO and $MgAl_2O_4$ layers, isolated secondary-phase inclusions were observed at the interface. The region marked by the dashed-line box in Fig. 2(a) shows a secondary phase inclusion adjacent to the MgO layer, which has different image characteristics from that of MgB_2. Chemical analysis by EDS and EELS, combined with structural analysis by Fourier-transform and HRTEM image simulations, reveals that this secondary phase has the MgB_4 structure. However, unlike the MgO and $MgAl_2O_4$ layers, MgB_4 layers are discontinuously distributed at the interface with very low population.

The formation of MgB_2 is believed to proceed through the diffusion of Mg vapor into the boron film, a process being analogous to that involved in the fabrication of MgB_2 wires.[12] Given that vapor pressure of Mg is approximately 50 Torr at 850 °C,[21] the MgB_2 phase would be thermodynamically stable according to the pressure-temperature-composition phase diagram calculated by Liu *et al.*[22] This is confirmed by our TEM observations in the present work. The formation of the intermediate epitaxial MgO layer is likely to be the result of a reaction between oxygen and magnesium during the course of annealing, or in part through the reaction of MgB_2 with oxygen. In the latter case, excess boron would likely further react with MgB_2, resulting in a formation of MgB_4, which agrees with the observation of small

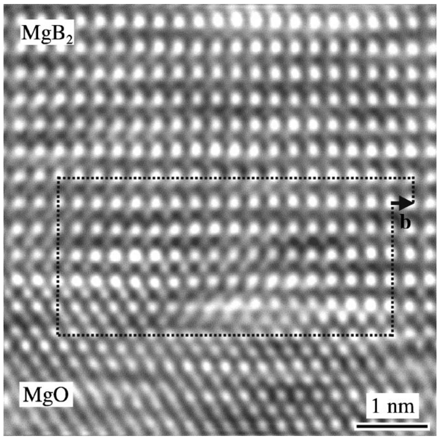

FIG. 4. HRTEM image of the MgB_2–MgO interface involving one partial edge misfit dislocation. Burgers vector of the dislocation is determined to be $\frac{1}{2}[1\bar{1}00]$ by the Burgers circuit as included in the figure.

MgB_4 inclusions adjacent to the MgO layer. However, the formation of epitaxial MgO prior to the growth of MgB_2 can not yet be completely ruled out. More experiments are underway to clarify this issue. The epitaxial $MgAl_2O_4$ is thus the product of solid state reaction between MgO and Al_2O_3, which was predominantly observed in MgO–Al_2O_3 system annealed at high temperature.[23,24] The formation of MgO phase at the interface between MgB_2 and Al_2O_3 substrate is energetically favorable due to the similarity of the oxygen sublattices in both MgO and Al_2O_3. Hence, the existence of oxygen plays a key role in developing the observed epitaxial MgO and $MgAl_2O_4$ at the interface. The oxygen may result from the quartz tube at high temperature and oxygen impurity in the sputtered B film.

Atomic structure of the MgB_2/MgO interface was examined by HRTEM combined with computer image simulations. Figure 3(a) is an HRTEM image of the MgB_2/MgO interface imaged with the electron beam incident along the $[11\bar{2}0]$ direction of MgB_2. The interface is sharp and clean. Computer simulated image that optimally fits the experimental image is inserted in the middle. The accordingly resolved atomic structure of the interface is schematically shown in Fig. 3(b). MgO has a cubic structure with space group $Fm\bar{3}m$ (No. 225) and lattice constant $a=4.220$ Å.[19] The in-plane alignment of $[1\bar{1}0]$ MgO with $[11\bar{2}0]$ MgB_2 results in a lattice mismatch of -3.3%. Thus, misfit dislocations were observed at the interface, essentially due to the lattice mismatch in the observed in-plane orientation relationship between MgB_2 and MgO. Figure 4 is a HRTEM image of the MgO–MgB_2 interface containing one dislocation. The Burgers vector, determined by the Burgers circuit shown as black lines in the image, is $\frac{1}{2}[1\bar{1}00]$ of MgB_2, which is a characteristic of partial misfit dislocation.

In conclusion, the microstructure and interfacial atomic structure of epitaxial MgB_2 thin films grown on the (0001) Al_2O_3 substrate have been studied by high-resolution transmission electron microscopy and analytical electron microscopy. Epitaxial MgO and $MgAl_2O_4$ layers were found between the MgB_2 film and the Al_2O_3 substrate, due to the presence of oxygen in the annealing process. The orientation relationships between these phases were determined to be $(0001)[11\bar{2}0]MgB_2//(111)[1\bar{1}0]MgO//(111)[1\bar{1}0]MgAl_2O_4//(0001)[10\bar{1}0]Al_2O_3$. The 30° angular off the *a*-to-*a* alignment between the basal plane of MgB_2 and Al_2O_3 results in a small lattice mismatch between the MgB_2 thin film and the (0001) Al_2O_3 substrate.

The authors gratefully acknowledge the financial support of the National Science Foundation through Grant Nos. DMR 9 875 405 (CAREER, X.Q.P.) and DMR/IMR 9 704 175. The work at the University of Wisconsin was supported by National Science Foundation through MRSEC for Nanostructure Materials.

[1] J. Nagamatsu, N. Nakagawa, T. Muranaka, Y. Zenitani, and J. Akimitsu, Nature (London) **410**, 63 (2001).
[2] R. J. Cava, Nature (London) **410**, 23 (2001).
[3] D. C. Larbalestier, L. D. Colley, M. Rikel, A. A. Polyanskii, J. Jiang, S. Patnaik, X. Y. Cai, D. M. Feldmann, A. Gurevich, A. A. Squitieri, M. T. Naus, C. B. Eom, E. E. Hellstrom, R. J. Cava, K. A. Regan, N. Rogado, M. A. Hayward, T. He, J. S. Slusky, P. Khalifah, K. Inumaru, and M. Haas, Nature (London) **410**, 186 (2001).
[4] D. K. Finnemore, J. E. Ostenson, S. L. Bud'ko, G. Lapertot, and P. C. Canfield, Phys. Rev. Lett. **86**, 2420 (2001).
[5] Y. Bugoslavsky, G. K. Perkins, X. Qi, L. F. Cohen, and A. D. Caplin, Nature (London) **410**, 563 (2001).
[6] T. B. Massalski, *Binary Alloy Phase Diagrams*, 2nd ed. (ASM International, Materials Park, Ohio, 1990) Vol. **1**, p. 499.
[7] H. M. Christen, H. Y. Zhai, C. Cantoni, M. Paranthaman, B. C. Sales, C. Rouleau, D. P. Norton, D. K. Christen, and D. H. Lowndes, Physica C **353**, 157 (2001).
[8] D. H. A. Blank, H. Hilgenkamp, A. Brinkman, D. Mijatovic, G. Rijnders, and H. Rogalla, Appl. Phys. Lett. **79**, 394 (2001).
[9] X. H. Zeng, A. Sukiasyan, X. X. Xi, Y. F. Hu, E. Wertz, W. Tian, H. P. Sun, X. Q. Pan, J. Lettieri, D. G. Schlom, C. O. Brubaker, Z. K. Liu, and Q. Li, Appl. Phys. Lett. **79**, 1840 (2001).
[10] S. R. Shinde, S. B. Ogale, R. L. Greene, T. Venkatesan, P. C. Canfield, S. L. Bud'ko, G. Lapertot, and C. Petrovic, Appl. Phys. Lett. **79**, 227 (2001).
[11] K. Ueda and M. Naito, Appl. Phys. Lett. **79**, 2046 (2001).
[12] C. B. Eom, M. K. Lee, J. H. Choi, L. J. Belenky, X. Song, L. D. Cooley, M. T. Naus, S. Patnaik, J. Jiang, M. Rikel, A. Polyanskii, A. Gurevich, X. Y. Cai, S. D. Bu, S. E. Babcock, E. E. Hellstrom, D. C. Larbalestier, N. Rogada, K. A. Regan, M. A. Hayward, T. He, J. S. Slusky, K. Inamura, M. K. Haas, and R. J. Cava, Nature (London) **411**, 558 (2001).
[13] P. C. Canfield, D. K. Finnemore, S. L. Bud'ko, J. E. Ostenson, G. Lapertot, C. E. Cunningham, and C. Petrovic, Phys. Rev. Lett. **86**, 2423 (2001).
[14] W. N. Kang, H. J. Kim, E. M. Choi, C. U. Jung, and S. I. Lee, Science **292**, 1521 (2001).
[15] M. Paranthaman, C. Cantoni, H. Y. Zhai, H. M. Christen, T. Aytug, S. Sathyamurthy, E. D. Specht, J. R. Thompson, D. H. Lowndes, H. R. Kerchner, and D. K. Christen, Appl. Phys. Lett. **78**, 3669 (2001).
[16] A. Berenov, Z. Lockman, X. Qi, J. L. MacManus-Driscoll, Y. Bugoslavsky, L. F. Cohen, M. H. Jo, N. A. Stelmashenko, V. N. Tsaneva, M. Kambara, N. H. Babu, D. A. Cardwell, and M. G. Blamire, Appl. Phys. Lett. **79**, 4001 (2001).
[17] C. B. Eom, MRS Falling Meeting, Boston, 2001.
[18] S. D. Bu, D. M. Kim, J. H. Choi, S. Patnaik, C. B. Eom, J. Lettieri, D. G. Schlom, W. Tian, and X. Q. Pan (unpublished).
[19] R. W. G. Wyackoff, *Crystal Structure* (Interscience, New York, 1953) Vol. 3.
[20] D. X. Li, P. Pirouz, A. H. Heuer, S. Yadavallis, and C. P. Flynn, Philos. Mag. A **65**, 403 (1992).
[21] A. N. Nesmeianov, *Vapor Pressure of the Chemical Elements* (Elsevier, Amsterdam, 1963), p. 176.
[22] Z. K. Liu, D. G. Schlom, Q. Li, and X. X. Xi, Appl. Phys. Lett. **78**, 3678 (2001).
[23] L. Navias, J. Am. Ceram. Soc. **44**, 434 (1961).
[24] C. B. Carter and H. Schmalzried, Phil. Mag. A **52**, 207 (1985).